Functional Morphometry of the Striatum in Parkinson's Disease on Three-Dimensional Surface Display of ^{123}I-β-CIT SPECT Data

Masanori Ichise, Yun J. Kim, Sean S. Erami, James R. Ballinger, Douglass Vines, Fumiko Tanaka and Anthony E. Lang

Division of Nuclear Medicine, Department of Medical Imaging, Mount Sinai Hospital, Toronto; Morton and Gloria Shulman Movement Disorders Center, Toronto; and University of Toronto, Toronto, Ontario, Canada

The purpose of this study was to evaluate whether striatal morphology on a three-dimensional surface display of ^{123}I–2β-carbomethoxy-3β-(4-iodophenyl)tropane (^{123}I-β-CIT) SPECT data can be used as a diagnostic index for Parkinson's disease. **Methods:** We studied 11 patients with mild Parkinson's disease and 21 age-matched controls. Triple-head SPECT scans were acquired for 30 min at 20 h after injection of ^{123}I-β-CIT. We measured the vertical height of the caudate head (H) and the length of the long axis of the striatum (L) on the three-dimensional surface display generated from SPECT data. The morphometric index of the striatum was defined as L/H. The power of L/H to discriminate Parkinson's disease and control groups was evaluated by discriminant function analysis and was compared with that of region of interest (ROI)-based ^{123}I-β-CIT binding measurements (V''_3) and their ratios. **Results:** The mean L/H ratios (ipsilateral/contralateral) to the most affected limbs were (33%/45%) lower in the Parkinson's disease group compared with the control group, respectively. All other ROI-based measures confirmed that dopamine transporter reductions were most severe in the contralateral posterior putamen (a 68% reduction in V''_3). In 1 patient with a subsequent clinical diagnosis of drug-induced parkinsonism, all SPECT measures were normal. The contralateral putamen contributed most to the discriminatory power, and the contralateral L/H showed the best discriminatory power of all SPECT measures. **Conclusion:** These results suggest that striatal morphology on a three-dimensional display of ^{123}I-β-CIT SPECT data provides information of diagnostic significance for Parkinson's disease. This morphometry can be done without requiring technically demanding ROI analysis, and thus this technique may be suitable for routine clinical use.

Key Words: ^{123}I-β-CIT; dopamine transporters; Parkinson's disease; dopamine SPECT; striatal morphometry

J Nucl Med 1999; 40:530–538

SPECT imaging of dopamine transporters using a cocaine analog, ^{123}I-2β-carbomethoxy-3β-(4-iodophenyl)tropane (β-CIT), has shown promise as a clinically useful tool to diagnose and evaluate patients with idiopathic Parkinson's disease (*1–3*). ^{123}I-β-CIT binds with high affinity to dopamine transporters located in the presynaptic terminals of the nigrostriatal dopamine neurons (*4*) and, therefore, is a marker of the neurons that degenerate in Parkinson's disease (*1*). ^{123}I-β-CIT SPECT studies have shown that not only is striatal ^{123}I-β-CIT binding reduced significantly in Parkinson's disease patients, but its reduction also is regionally uneven in two ways (*1–3*). First, dopamine transporter binding shows lateralized differences, being more reduced in the striatum contralateral to the clinically more affected side. Second, it is more reduced in the putamen than in the caudate within the same striatum (*2,3*). These findings are consistent with those of pathological studies of Parkinson's disease, namely, the substantia nigra degenerates asymmetrically between the two sides, and the ventrolateral substantia nigra projecting to putamen degenerates more severely than the ventromedial striatum projecting to caudate (*5,6*). In addition, ^{123}I-β-CIT SPECT may be sensitive enough to detect subclinical involvement of dopamine projections in Parkinson's disease (*3*), because 40%–50% losses of these projections are said to occur before patients develop parkinsonian symptoms (*6*). Given the widespread availability of SPECT, this technique may become a cost-effective clinical tool for the evaluation of Parkinson's disease patients.

^{123}I-β-CIT provides excellent image quality with high target-to-background ratios as a result of its low nonspecific binding and high affinity for dopamine transporters (*7*). However, for SPECT imaging of dopamine transporters to be useful, readily accessible and accurate methods are needed to extract information about the striatal density of dopamine transporters from image data. SPECT measurement of the specific-to-nondisplaceable tissue ratio from a short scan during 18–24 h after a bolus injection of ^{123}I-β-CIT provides a measure ($V''_3 = B_{max}/K_D V_2$) that reflects the density of dopamine transporters (B_{max}) (*7*).

Although this quantification method is relatively straightforward, it requires accurate ways to define and place regions of interest (ROIs) to measure tracer activities in both the striatum and reference tissue. This ROI analysis can be

Received Apr. 17, 1998; revision accepted Sep. 15, 1998.

For correspondence or reprints contact: Masanori Ichise, MD, Rm. 635, Nuclear Medicine, Mount Sinai Hospital, 600 University Ave., Toronto, Ontario, Canada M5G 1X5.

technically demanding and time-consuming for routine clinical use. Any alternative methods that do not rely on ROI analysis should facilitate the routine clinical use of ^{123}I-β-CIT SPECT. Because the reduction of ^{123}I-β-CIT binding in Parkinson's disease appears characteristically uneven within the striatum (*2,3*), striatal topography of dopamine transporter distribution may provide diagnostically significant information. Furthermore, because this topographic unevenness is characterized by the relative differences of ^{123}I-β-CIT activity within the striatum, this information may be obtained by using alternative methods that do not rely on ROI analysis.

In this study, the vertical height of caudate head and the length of the long axis of the striatum on a three-dimensional surface display of ^{123}I-β-CIT SPECT data were measured, because these measurements do not require traditional ROI analysis. The ratio of these two measurements was then evaluated as a potential diagnostic index for Parkinson's disease. To this end, the ability of this morphometric index to discriminate between Parkinson's disease patients and healthy controls was compared with that of detailed dopamine transporter binding measurements (V''_3) and their lateralized asymmetry index as well as their intrastriatal ratios.

MATERIALS AND METHODS

Subjects

Eleven patients with Parkinson's disease (6 men, 5 women; mean age 61.5 ± 8.3 y; age range 51–74 y) were recruited from referrals to the Movement Disorders Clinic at the Toronto Hospital. Selection criteria included patients with clinically mild Parkinson's disease, as assessed by the Hoehn and Yahr Scale (Stage ≤2.5) and the Unified Parkinson's Disease Rating Scale (UPDRS) (*8*) (total UPDRS scores = 25.8 ± 10.7), who were in the early course of their illness (duration 3.1 ± 2.9 y) (Table 1). Diagnosis of Parkinson's disease was made according to the UK Parkinson's Disease Brain Bank clinical diagnostic criteria (*9*). Patients with dementia and other major neuropsychiatric disorders were excluded. Four were drug-naive, 1 took levodopa plus selegiline and the remaining 6 took nondopamimetic antiparkinsonian medication (Table 1). Those on drug treatment discontinued their drugs for at least 12 h before commencement and until completion of the ^{123}I-β-CIT SPECT studies. All UPDRS scores shown in Table 1 were obtained before SPECT studies, when the drug-treated patients had been off medication for at least 12 h.

One patient (patient 4, Table 1) stands apart from the other patients in that the diagnosis of Parkinson's disease in this patient subsequently has been refuted. At the time of recruitment, this patient had mild but definite parkinsonian features (rest tremor and rigidity). In retrospect, however, these may have been due to previous flunarizine use as part of migraine therapy for 2 y, which the patient had discontinued 1 mo before initial evaluation. On follow-up 4 mo after SPECT scans (performed 1.5 y after flunarizine withdrawal), neurological examination revealed only questionable reduction in right-arm swing and a mild postural tremor but no other abnormalities. Therefore, although this patient was classified as having Parkinson's disease and was included in this study, the diagnosis was not supported on subsequent clinical evaluation, the subsequent diagnosis being flunarizine-induced parkinsonism.

Twenty-one mean-age-matched healthy subjects (12 men, 9 women; mean age 65.8 ± 9.6 y; age range 48–83 y) served as controls. None of the controls had a current or past history of neuropsychiatric disorders or a family history of movement disorders, based on a screening interview. All were free of drugs for at least 3 mo before the study. All control subjects had normal MRI of the head, normal electroencephalogram and normal Mini Mental Status Examination (*10*). These control subjects were evaluated for extrapyramidal motor function by using Part III (motor) of the UPDRS. None had significant extrapyramidal deficits as determined by previously published criteria (resting tremor ≥1 and/or rigidity ≥2) (*11*). All patients and healthy subjects gave written informed consent. The project was approved by the Human Subjects Review Committee of the University of Toronto.

TABLE 1
Demographic Characteristics of Patients with Parkinson's Disease

Patient no.	Sex	Age (y)	Duration (y)*	H & Y stage	UPDRS		Medication (total daily dose in mg)
					Total	Motor	
1	M	51	4	2	29	23	Selegiline (10)
2	M	51	1	2	24.5	21	Selegiline (10)/trihexyphenidyl (6)
3	M	53	1	1	10.5	8	None
4	M	53	2	2	9.5	8.5	Selegiline (10)
5	M	61	2	2	21	13.5	None
6	M	66	2.5	2.5	19.5	14	Selegiline (10)
7	F	63	10	2	33.5	26.5	Amantadine (200)
8	F	65	3	2.5	33.5	26	None
9	F	67	1	2	23	17.5	Amantadine (200)
10	F	72	7	2	45	23	Sinemet (600)/selegiline (10)
11	F	74	1	2.5	35	24.5	None
	Mean	61.5	3.1	2.0	25.8	18.7	
	SD	8.3	2.9	0.4	10.7	6.8	

*Disease duration.
H & Y = Hoehn and Yahr stage; UPDRS = Unified Parkinson's Disease Rating Scale.

Labeling of ^{123}I-β-CIT

Labeling of ^{123}I-β-CIT was performed using the corresponding trimethylstannyl precursor and ^{123}I-NaI as described previously (*12*). The radiochemical yield was 54.9% ± 11.1%, and the radiochemical purity was 98.3% ± 1.8%. Retrospective sterility testing was negative.

SPECT Imaging

Imaging was performed using a triple-head SPECT system (Prism 3000XP; Picker International, Inc., Cleveland, OH) equipped with high-resolution fanbeam collimators and interfaced to a dedicated computer (Odyssey VP; Picker International, Inc., Cleveland, OH). Scans were acquired every 5 min for 30 min, beginning at 20 ± 1.5 h after a bolus intravenous injection of 254 ± 64 MBq ^{123}I-β-CIT. For each scan, 120 7.5-s projection images were obtained using 3°-angle intervals on a 128 × 128 matrix over 360° by rotating each head 120°. The radius of rotation was fixed at 13.5 cm. Four fiducial markers containing 1.5 μCi ^{99m}Tc were taped, two on each side of the subject's head, at the level of the canthomeatal line (CML). Full width at half maximum of the system was 11.2 mm in water at the center of the field of view. The mean sensitivity of the system was 994 ± 24 cpm/μCi and varied less than 1.6% and 2.5% within and between the experiments, respectively. Before the ^{123}I-β-CIT study, subjects were given 400 mg of potassium perchlorate orally.

SPECT images were reconstructed on a 128 × 128 matrix. One-pixel-thick (2.17-mm) transaxial slices from the vertex of the brain to the level of the CML, as identified by the fiducial markers, were reconstructed parallel to the CML using a three-dimensional Butterworth postreconstruction filter (order 10, cutoff frequency 0.25 cycles/pixel), after applying a ramp backprojection filter. Attenuation correction was performed by assuming uniform attenuation equal to that of water ($\mu = 0.15\ cm^{-1}$) within an ellipse drawn around the skull, as identified by the fiducial markers.

Image Data Analysis

To obtain an index that reflects the topographic distribution of ^{123}I-β-CIT activity within the striatum without resorting to ROI analysis, the greatest vertical height of the caudate head (H) and the greatest length of the long axis of the striatum (L) on the three-dimensional surface display of ^{123}I-β-CIT SPECT data were measured (Fig. 1A). The morphometric index of the striatum was defined as L/H. The three-dimensional surface images were generated from transaxial SPECT data using the previously described method (*13*). In our preliminary evaluation of L/H measurements at predefined three-dimensional surface threshold values (40%–70% in 5% increments), the L/H ratio was relatively stable across the different threshold values (Fig. 2A), and the threshold values between 50% and 60% resulted in maximum (26%) and minimum (6%) values of intersubject coefficients of variation in L/H measurements in the patients and controls, respectively (Fig. 2B). The surface threshold value was therefore set at 55% in this study. This threshold value of 55% generated three-dimensional surface images consisting of only the dopamine transporter signal from the striatum, eliminating the serotonin transporter signal from the thalamic or midbrain region.

To compare the power of L/H to discriminate between Parkinson's disease patients and control groups with that of traditional ROI-based measurements, we measured the ^{123}I-β-CIT binding parameter (V''_3), lateralized V''_3, asymmetry index (AI) and two intrastriatal V''_3 ratios, anterior putamen-to-caudate (AP/CD) and posterior putamen-to-caudate (PP/CD) V''_3 ratios. CD, AP and PP

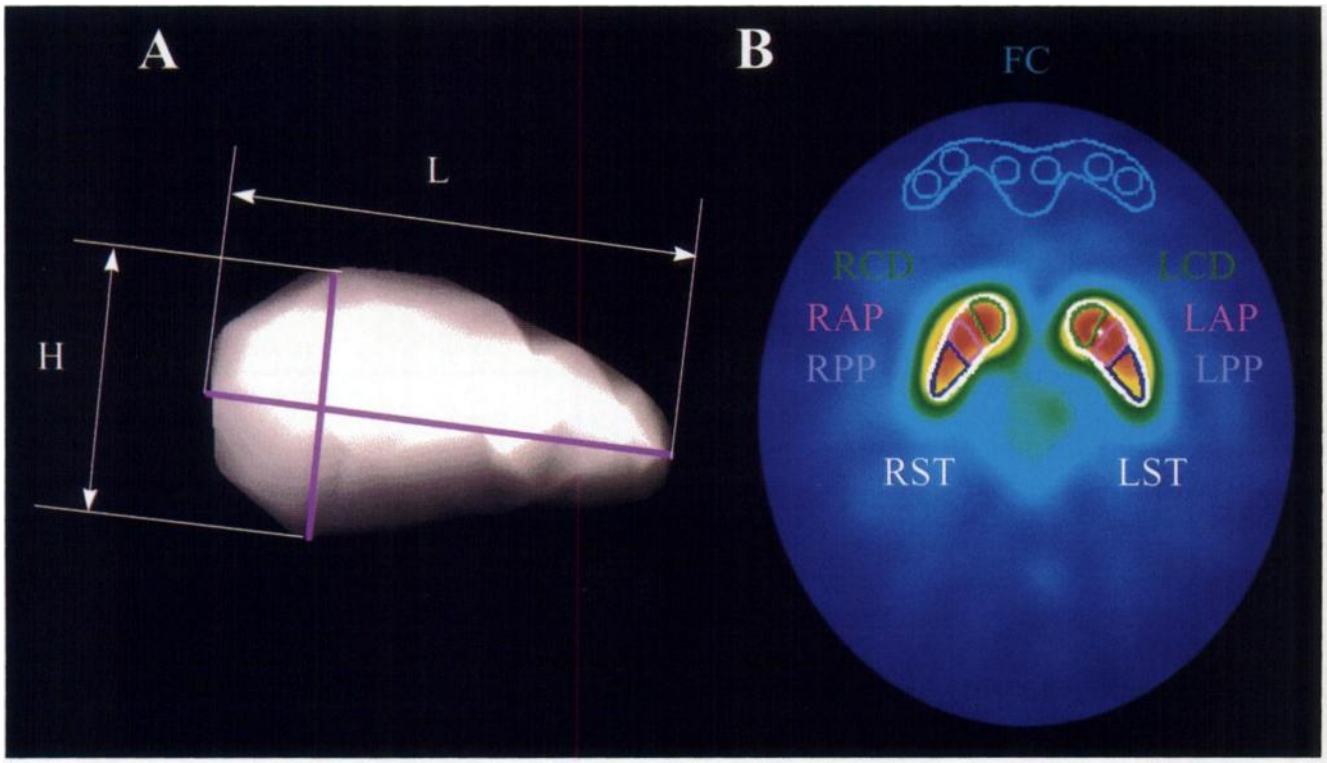

FIGURE 1. (A) Three-dimensional surface display of left striatum shows typical vertical height (H) of caudate head and length (L) of long axis of striatum (lateral oblique view). (B) Transverse ^{123}I-β-CIT SPECT image shows typical ROI sets. R = right; L = left; FC = frontal cortex; ST = striatum; CD = caudate; AP = anterior putamen; PP = posterior putamen.

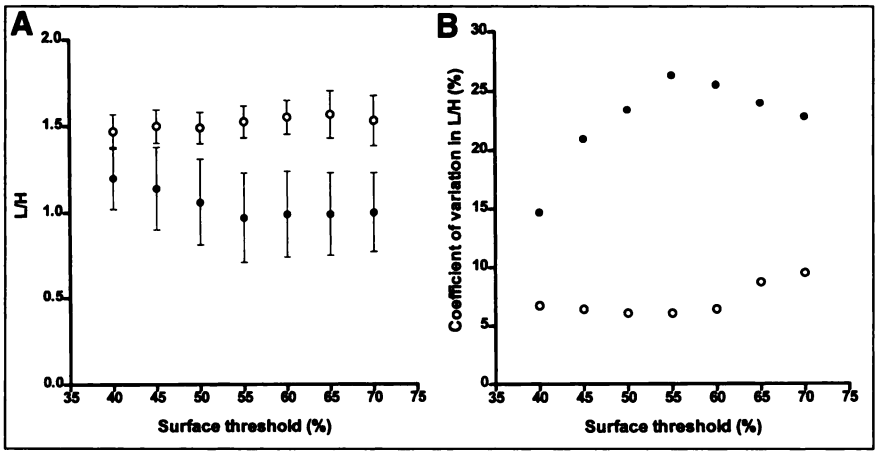

FIGURE 2. Plots of three-dimensional surface threshold values versus mean morphometric index (L/H) values (A) and coefficients of variation in L/H (B), respectively. Healthy subjects and patients are shown in hollow and solid circles, respectively. Error bars indicate SD.

were measured separately, because postmortem study has indicated that within the striatum there is also an uneven topographic gradient of dopamine loss in which the posterior putamen is more severely affected than the anterior putamen, which is in turn more affected than the caudate (*14*). V''_3 was calculated as the specific-to-nondisplaceable ^{123}I-β-CIT activity ratio using the frontal cortex as the nondisplaceable region, according to the method described previously (*7*). AI was defined as the difference of V''_3 values between ipsilateral and contralateral sides, expressed as percentage of the mean of the two. For the patient group, "contralateral" was defined as the side contralateral to the most affected limbs or the side showing the lowest V''_3 values when the limbs were affected equally on both sides. For control subjects, "contralateral" was arbitrarily assigned to the left side on the basis of our normal control data, which showed no significant lateralized differences in the outcome measures, L/H, V''_3 or intrastriatal V''_3 ratios.

To measure V''_3 for CD, AP and PP separately, ROIs were defined and placed by using a modification of our previously reported method (*15*). The modification consisted of placing two separate ROIs for putamen and six small ROIs fitted within the reference ROI (frontal cortex), the latter to improve count losses from partial volume effects. In brief, ROIs were placed using predefined templates on a summed image (0.868 cm thick) through the middle of the striatum in two steps (Fig. 1B). First, ROIs were placed over the whole striatum (volume 3.00 cm^3) in each hemisphere and the frontal cortex (volume 8.85 cm^3), respectively. Second, ROIs for three striatal subregions, CD head (volume 0.83 cm^3), AP (volume 0.66 cm^3) and PP (volume 0.94 cm^3), were fitted within the striatum, and six circular ROIs (total volume 3.00 cm^3) were fitted within the frontal cortex. ROI placement was aided by the stereotactic brain atlas (*16*). To eliminate interoperator variation, the same individual applied all ROIs. The mean coefficient of intraoperator variability in the measurement of V''_3 was 3.3% ± 0.6%.

Statistical Analysis

The single patient (patient 4) in whom drug-induced parkinsonism was subsequently diagnosed was excluded from the statistical analyses. Because all 15 outcome measures, namely, L/H, V''_3 (CD, AP and PP), AI (CD, AP and PP) and intrastriatal V''_3 ratios (AP/CD and PP/CD), each set consisting of ipsilateral and contralateral except for AI, were normally distributed (Kolmogorov-Smirnov test for normality, $P > 0.10$), parametric statistical tests were used in this study. Hotelling's T^2 (a multivariate test) and 2-tailed Student t tests for unpaired samples were performed to compare the 15 outcome measures between the Parkinson's disease and control groups. Two-tailed Student t tests for paired samples were performed for within-group comparisons of outcome measures between ipsilateral and contralateral sides and between ipsilateral or contralateral substriatal regions, respectively. Multiple t test comparisons were corrected by Bonferroni's method. The power of each outcome measure to discriminate between patient and control groups was evaluated by calculating partial Wilks λ by performing discriminant function analysis (*17*). This statistic is an estimate of the unique contribution of the respective variable to the discrimination between groups. Lower values of partial Wilks λ denote a more unique discriminatory contribution. Additionally, discriminant function analysis was used for post hoc predictive classification of the group membership of cases. Those UPDRS motor scores that pertain to extremities were separated into ipsilateral and contralateral sides. The relationships between SPECT measures (L/H, V''_3 and intrastriatal V''_3 ratios) and these lateralized motor UPDRS scores were determined by linear regression analysis. Statistical significance was defined as $P < 0.05$. Summaries of study variables were expressed as mean ± SD. All statistical analyses were implemented in STATISTICA (StatSoft, Inc., Tulsa, OK).

RESULTS

The group of patients with Parkinson's disease (excluding patient 4) and the control group were significantly different in their overall outcome measures ($F_{15,15} = 75$, $T^2 = 2178$, $P < 10^{-5}$, Hotelling's T^2) and all 15 t tests showed significantly different mean outcome measure values in the group with Parkinson's disease compared with the control group ($P < 10^{-3}$). A summary of the mean values of all outcome measures in the Parkinson's disease and control groups is shown in Table 2. The mean L/H ratios (ipsilateral/contralateral) were (33%/45%) lower in the Parkinson's disease group than in the control group, respectively ($P < 10^{-5}$), with the contralateral side showing more reductions compared with the ipsilateral side ($P < 0.05$).

The mean V''_3 values (ipsilateral/contralateral) for CD, AP and PP were (32%/43%), (43%/51%) and (60%/68%) lower in patients with Parkinson's disease than in the control group, respectively ($P < 10^{-4}$). These reductions in the mean V''_3 values were more marked in the contralateral side

TABLE 2

^{123}I-β-CIT SPECT Outcome Measures and Discriminant Function Analyses in Patients with Parkinson's Disease and Healthy Control Subjects*

	Morphometric index (L/H)		V''_3						Lateralized V''_3 asymmetry index (AI)			Intrastriatal V''_3 ratio			
			CD		AP		PP					AP/CD		PP/CD	
	Ipsi	Contra	Ipsi	Contra	Ipsi	Contra	Ipsi	Contra	CD	AP	PP	Ipsi	Contra	Ipsi	Contra
Patients	1.03	0.84	4.51	3.78	4.07	3.59	2.42	1.93	17.4	12.4	21.6	0.91	0.95	0.55	0.52
± SD	± 0.29	± 0.14	± 1.09	± 0.88	± 1.03	± 0.83	± 0.65	± 0.38	± 9.8	± 11.8	± 21.9	± 0.06	± 0.06	± 0.10	± 0.08
Controls	1.53	1.52	6.63	6.68	7.13	7.38	6.02	6.11	−0.8	−3.5	−1.6	1.08	1.11	0.91	0.92
± SD	± 0.13	± 0.09	± 0.83	± 0.80	± 0.87	± 0.89	± 0.85	± 0.78	± 5.2	± 7.8	± 5.1	± 0.06	± 0.05	± 0.06	± 0.06
t	6.8	16.4	6.0	9.2	8.6	11.3	11.8	16.0	−6.8	−4.5	−4.7	7.5	7.8	12.5	15.0
P†	$<10^{-5}$	$<10^{-5}$	$<10^{-4}$	$<10^{-5}$	$<10^{-5}$	$<10^{-5}$	$<10^{-5}$	$<10^{-5}$	$<10^{-5}$	$<10^{-3}$	$<10^{-3}$	$<10^{-3}$	$<10^{-5}$	$<10^{-5}$	$<10^{-5}$
Partial Wilks λ	0.387	0.098	0.446	0.256	0.281	0.185	0.172	0.102	0.388	0.592	0.570	0.337	0.325	0.157	0.114
Correct classification	90%	100%	94%	97%	94%	100%	100%	100%	90%	90%	84%	94%	97%	97%	100%

*Patient 4 was not included in summary of mean values of all outcome measures.

†Two-tailed significance for between-group comparison after Bonferroni's correction.

L/H = striatal length/caudate height; CD = caudate; AP = anterior putamen; PP = posterior putamen; ipsi = ipsilateral; contra = contralateral (ipsilateral for controls was arbitrarily assigned to right striatum).

than in the ipsilateral side ($P < 0.05$). These lateralized differences were reflected in the higher mean AI values for the Parkinson's disease group (all positive) compared with the control group ($P < 10^{-3}$). In addition, the mean reductions of V''_3 in the PP of patients with Parkinson's disease were more marked than in the AP, and the mean reductions of V''_3 in the latter in turn were more marked than in the CD on both ipsilateral and contralateral sides ($P < 10^{-3}$). Decreased ^{123}I-β-CIT activity, particularly in the contralateral putamen of a patient with Parkinson's disease (patient 3) is illustrated in Figure 3 (top row), using selected three-dimensional surface display and tomographic images, contrasted with the corresponding images (bottom row) of an age-matched control.

The mean AP/CD (ipsilateral/contralateral) and PP/CD (ipsilateral/contralateral) V''_3 ratios were (16%/14%) and (40%/43%) lower in the group with Parkinson's disease than in the control group, respectively ($P < 10^{-3}$). Although there were no significant lateralized differences in the mean reductions of these intrastriatal V''_3 ratios ($P > 0.4$), the mean reductions in PP/CD were more marked compared with AP/CD for both ipsilateral and contralateral sides ($P < 10^{-5}$). In the control group, there were no lateralized differences of L/H, V''_3 or intrastriatal V''_3 ratios ($P > 0.06$).

In all patients excluding 1 (patient 4), 7 (contralateral L/H, contralateral CD V''_3, contralateral AP V''_3, PP V''_3 bilaterally and PP/CD V''_3 ratios bilaterally) were all below the control range. In contrast, the remaining outcome measures showed overlap with the control group (Figs. 4 and 5). In patient 4, with the subsequent clinical diagnosis of drug-induced parkinsonism, all outcome measures were within the control range (Figs. 4 and 5).

All discriminant function analyses were highly significant (F values ranging from 20 to 268 and $P < 10^{-4}$ for all subjects, Table 2). The partial Wilks λ values ranged from 0.098 to 0.592, and the percentage values of subjects correctly classified into the respective groups ranged from 84% to 100%, indicating relatively good ability of all outcome measures to discriminate between the Parkinson's disease and control groups (Table 2). In particular, the discriminatory powers of contralateral L/H, contralateral PP V''_3, contralateral PP/CD V''_3 ratio, ipsilateral PP V''_3 and contralateral AP V''_3, in the order of decreasing discriminatory power (or increasing values of Wilks λ, Table 2), were excellent, with 100% of subjects correctly classified post hoc into the respective groups. On the other hand, AI showed the least discriminatory power (84%–90% of subjects were correctly classified into the respective groups, Table 2), and the discriminatory power of the remaining measures was intermediate to the other two. Thus, the contralateral putamen contributed most to the discriminatory power, which was well reflected in the measure, L/H. The contralateral L/H, in fact, showed the best discriminatory power of all outcome measures.

The lateralized motor UPDRS scores negatively correlated with V''_3 measures for all three striatal subregions, CD

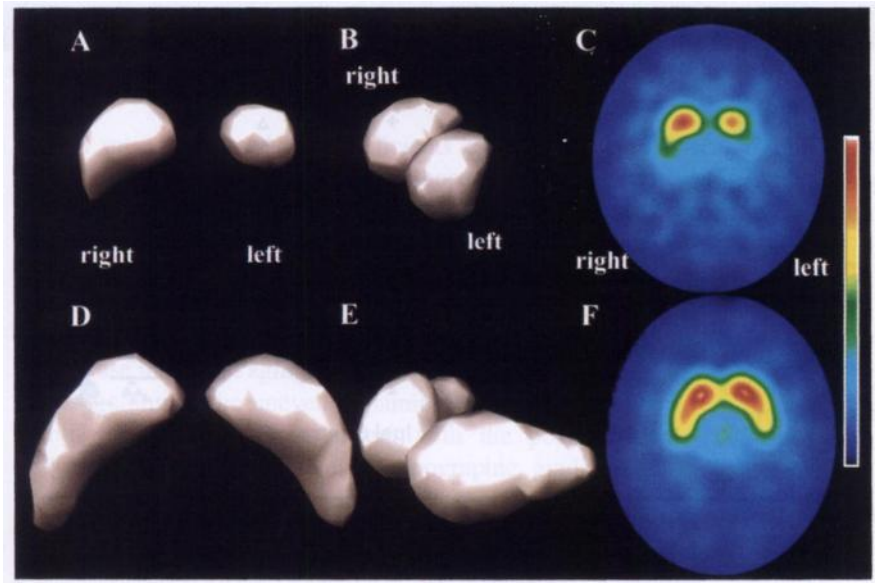

FIGURE 3. Three-dimensional surface displays (A, B, D and E) and ^{123}I-β-CIT SPECT images (C and F) of 53-y-old patient with Parkinson's disease (top row) and age-matched healthy individual (bottom row). Surface displays demonstrate truncation of putamen, degree being more marked on left than right for patient (A and B) compared with healthy subject (D and E). Patient (patient 3) had clinically unilateral parkinsonism. Patient's topographical abnormalities of striatum are also apparent on SPECT image (C).

($r = -0.50$, $P = 0.03$), AP ($r = -0.46$, $P = 0.04$) and PP ($r = -0.59$, $P = 0.007$). There was a trend toward a similar linear relationship between the lateralized UPDRS scores and the L/H measure, but this did not reach statistical significance ($r = -0.40$, $P = 0.08$). On the other hand, there was no significant correlation between the lateralized UPDRS and intrastriatal V''_3 measures.

DISCUSSION

The results of this study demonstrated that the ratio of morphological dimensions of the striatum measured on a three-dimensional display of ^{123}I-β-CIT SPECT data can be used to discriminate between patients with early Parkinson's disease and healthy controls. The discriminatory power of this morphometric index of the striatum derives from the characteristic reductions of ^{123}I-β-CIT binding in the contralateral putamen of patients with Parkinson's disease. Because the three-dimensional surface displays were generated from ^{123}I-β-CIT SPECT data acquired during the protracted equilibrium phase, the only known major factor that influences this morphometric index is the dopamine transporter density gradient between the CD and putamen. The method presented here provides information on the uneven intrastriatal topography of dopamine transporter binding without requiring traditional ROI analysis. Therefore, this simple approach may facilitate the routine use of ^{123}I-β-CIT SPECT as a tool to aid accurate diagnosis and evaluation of patients with Parkinson's disease.

The accurate diagnosis of Parkinson's disease is important not only for counseling and management of patients but also in conducting pharmacological and epidemiological studies. Traditionally, diagnosis of Parkinson's disease has been clinical. However, in the detailed clinico-pathological study reported by Hughes et al. (*9*), 24 of 100 cases with an antemortem clinical diagnosis of typical Parkinson's disease were found to have other diseases at postmortem examination. Conversely, patients with atypical clinical features may turn out to have typical pathological findings of Parkinson's disease (*18*). Therefore, any tests that can reduce diagnostic inaccuracy should have an important effect not only on practical management of patients with Parkinson's disease but also on progress in research on Parkinson's disease,

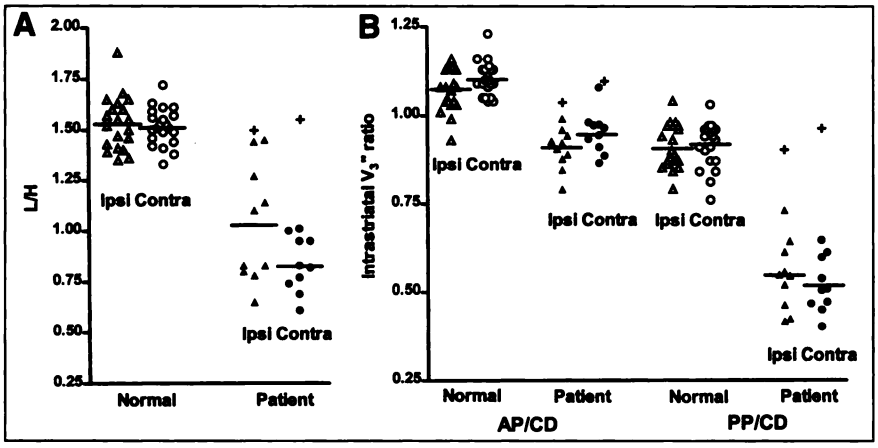

FIGURE 4. Scatter diagrams of individual values of L/H (A) and intrastriatal V''_3 ratios (B) for Parkinson's disease patients compared with healthy subjects. L/H = striatal length/caudate height; AP/CD = anterior putamen/caudate; PP/CD = posterior putamen/caudate; ipsi = ipsilateral; contra = contralateral. Healthy subjects and patients are indicated by hollow and solid symbols, respectively. + indicates values for patient 4, who had drug-induced parkinsonism. Horizontal bars indicate mean value for respective group.

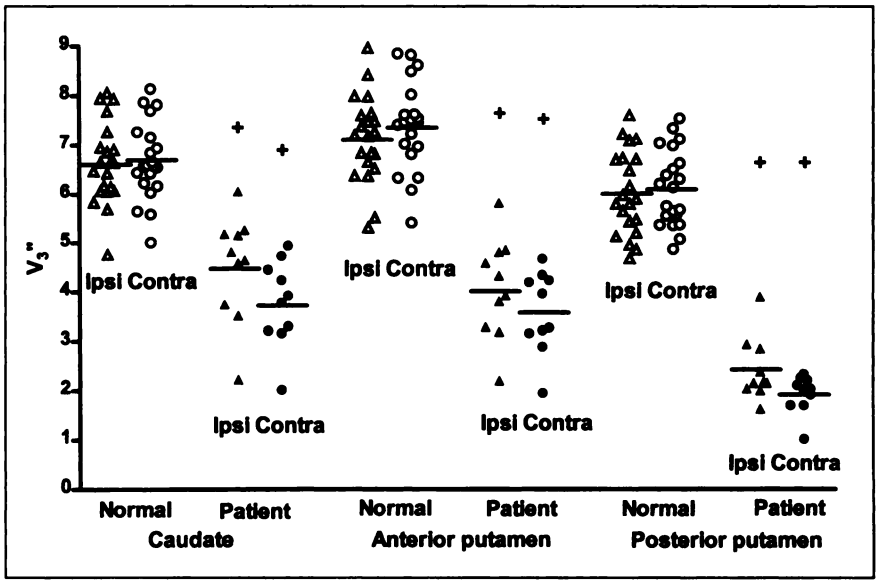

FIGURE 5. Scatter diagram of individual ^{123}I-β-CIT binding (V''_3) values in CD, AP and PP of Parkinson's disease patients compared with healthy subjects. Ipsi = ipsilateral; contra = contralateral. Healthy subjects and patients are indicated by hollow and solid symbols, respectively. + indicates values for patient 4, who had drug-induced parkinsonism. Horizontal bars indicate mean value for respective group.

especially if the test can be made widely available. This study, as well as those of others (*1–3*), suggests that SPECT imaging of dopamine transporters may serve as one such test, although the ultimate accuracy of SPECT scan diagnosis of Parkinson's disease must be evaluated against the pathological diagnosis.

The clinically misdiagnosed cases in the studies reported by Hughes et al. (*9*) and Rajput et al. (*19*) included cases of progressive supranuclear palsy (PSP), multiple system atrophy (MSA), Alzheimer's disease, Alzheimer-type pathology, vascular disease, essential tremor, drug-induced parkinsonism and others. Previous ^{123}I-β-CIT SPECT studies have shown that striatal dopamine transporter binding is also decreased in patients with PSP or MSA (*20,21*). On the other hand, SPECT studies using ^{123}I-iodobenzamide have shown reductions in striatal dopamine D2 receptor binding in patients with PSP or MSA (*22*) but no such reductions in patients with Parkinson's disease (*23*). Therefore, SPECT imaging of dopamine D2 receptors may be a promising complementary technique for the differential diagnosis of parkinsonism.

Of interest in this study is the 1 patient (patient 4) in whom all ^{123}I-β-CIT imaging measures were normal. This patient also had normal SPECT imaging of D2 receptors using ^{123}I-iodobenzofuran at our institution (data not shown). Subsequent clinical evaluation, supported by the SPECT scan results, caused us to refute the original diagnosis of Parkinson's disease in this patient. The patient probably had flunarizine-induced parkinsonism. He continues to demonstrate a postural tremor. It has been suggested that preexisting essential tremor may predispose individuals to the parkinsonism induced by this class of drugs (*24*). In drug-induced parkinsonism, the presynaptic dopamine pathways are expected to be intact unless complicated by underlying nigral dysfunction (*25*). Therefore, the experience of this case emphasizes the potential value of this imaging tool in the diagnosis of Parkinson's disease.

These findings of decreased striatal V''_3 values, particularly in the contralateral putamen of patients with Parkinson's disease compared with normals, as measured by ^{123}I-β-CIT SPECT, confirm those of others (*2,3*). In our patients, the mean V''_3 values for contralateral CD, AP and PP were 3.78, 3.59 and 1.93, respectively. These values generally agree with those reported by Seibyl et al. (*2*) (CD = 4.71 and putamen = 2.29, contralaterally, using a single ROI for putamen). However, our slightly lower V''_3 values, despite the fact that the mean ages of patients in the two studies were similar (62 y versus 63 y) and our patients were milder in their clinical severity than those in the latter study, probably are the result of methodological differences between the two studies. Specifically, ROI size significantly affects the magnitude of V''_3 measurements as a result of differences in partial volume effects, as we previously reported for ^{123}I-iodobenzofuran dopamine D2 receptor SPECT imaging (*15*). Therefore, another advantage of the use of three-dimensional displays may be their independence from ROI size. However, the morphometric technique described in this study is probably of limited use in certain other causes of parkinsonism, such as PSP, in which the changes in the dopamine projections to the striatum are more uniformly affected (*26*). In addition, this morphometric analysis may be complicated in the evaluation of patients with Parkinson's disease with mesencephalic tissue implantation, in which striatal dopamine transporters result in patchy increases.

Another important factor in comparing ^{123}I-β-CIT binding measurements between patients and controls is the age effects of these measurements. ^{123}I-β-CIT binding has been shown to decline with increasing age (*27*). This will contribute to the intersubject variability of V''_3 measurements. In this study, the intersubject variability of V''_3 for the

control group expressed as coefficients of variation were significantly larger (11%–13%) than those of L/H (6%) and the intrastriatal V''_3 ratios (4%–6%). These differences suggest that the age effects on V''_3 may be similar across the striatal subregions and may contribute to the slightly greater discriminatory power of L/H and intrastriatal V''_3 ratios compared with V''_3 in this study. However, the L/H may be of limited use in normal aging studies.

Our finding of the uneven dopamine transporter deficits within the putamen is consistent with the postmortem finding that there is an uneven topographic gradient of dopamine loss, the PP being more severely affected than the AP (*14*). Morrish et al. (*28*) reported a detailed in vivo study to investigate regional changes in dopamine metabolism within the striatum with clinical progression of Parkinson's disease, using coregistration of ^{18}F-dopa PET and MRI. These investigators found that dopamine metabolism in the putamen decreases with increasing clinical severity, the regional pattern of deficits within the putamen progressing along the dorso-ventral as well as the caudo-rostral gradients. Thus, early in the disease course, dopamine metabolism is focally decreased in the most posterior (dorso-caudal) portion of the putamen. As clinical severity increases, loss of focal dopamine metabolism spreads in the ventral and rostral (anterior) direction. In this study, however, there was no significant correlation between the clinical severity (the lateralized UPDRS score) and our morphometric index, although there was a trend toward a linear relationship. On the other hand, the lateralized motor UPDRS scores negatively correlated with V''_3 measures for all three striatal subregions, which is consistent with the finding of the ^{123}I-β-CIT SPECT study reported by Seibyl et al. (*2*). Therefore, the use of the L/H ratio in longitudinal disease progression studies may be limited, although it appears promising as a diagnostic tool for Parkinson's disease. In addition, the findings reported by Morrish et al. (*28*) suggest that more detailed topographical analyses of the striatum on ^{123}I-β-CIT SPECT than reported in this study, preferably incorporating coregistered MRI-defined striatal morphology, may also predict the underlying clinical severity of Parkinson's disease, which is typically masked by the symptomatic effects of antiparkinsonian medication.

CONCLUSION

Striatal morphology on a three-dimensional display of ^{123}I-β-CIT SPECT data provides information of diagnostic significance for Parkinson's disease. This morphometry can be done without requiring technically demanding ROI analysis, and thus this technique may be suitable for routine clinical use.

ACKNOWLEDGMENTS

This study was supported by a grant from the Medical Research Council of Canada (HT-13367); the SPECT Research Fund from the Department of Medical Imaging, Mount Sinai Hospital; Picker International Canada, Inc.; and the National Parkinson Foundation (Miami, FL).

REFERENCES

1. Innis RB, Seibyl JP, Scanley BE, et al. Single photon emission computed tomographic imaging demonstrates loss of striatal dopamine transporters in Parkinson disease. *Proc Natl Acad Sci USA.* 1993;90:11965–11969.
2. Seibyl JP, Marek KL, Quinlan D, et al. Decreased single-photon emission computed tomographic [^{123}I]β-CIT striatal uptake correlates with symptom severity in Parkinson's disease. *Ann Neurol.* 1995;38:589–598.
3. Marek KL, Seibyl JP, Zoghbi SS, et al. [^{123}I]β-CIT/SPECT imaging demonstrates bilateral loss of dopamine transporters in hemi-Parkinson's disease. *Neurology.* 1996;46:231–237.
4. Neumeyer JL, Wang SY, Milius RA, et al. [^{123}I]-2 β-carbomethoxy-3 β-(4-iodophenyl) tropane: high-affinity SPECT radiotracer of monoamine reuptake sites in brain. *J Med Chem.* 1991;34:3144–3146.
5. German DC, Manaye K, Smith WK, Woodward DJ, Saper CB. Midbrain dopaminergic cell loss in Parkinson's disease: computer visualization. *Ann Neurol.* 1989;26:507–514.
6. Fearnley JM, Lees AJ. Aging and Parkinson's disease: substantia nigra regional selectivity. *Brain.* 1991;114:2283–2301.
7. Laruelle M, Wallace E, Seibyl JP, et al. Graphical, kinetic, and equilibrium analyses of in vivo [^{123}I]β-CIT binding to dopamine transporters in healthy human subjects. *J Cereb Blood Flow Metab.* 1994;14:982–994.
8. Fahn S, Shoulson I. *Unified Rating Scale for Parkinsonism. The Parkinson Study Group.* Florsham Park, NJ: MacMillan; 1987:153–163.
9. Hughes AJ, Daniel SE, Kilford L, Lees AJ. Accuracy of clinical diagnosis of idiopathic Parkinson's disease: a clinico-pathological study of 100 cases. *J Neurol Neurosurg Psychiatry.* 1992;55:181–184.
10. Folstein MF, Folstein SE, McHugh PR. "Mini-mental state." A practical method for grading the cognitive state of patients for the clinician. *J Psychiatry Res.* 1975;12:189–198.
11. Francis PT, Sims NR, Procter AW, Bowen DM. Cortical pyramidal neurone loss may cause glutamatergic hypoactivity and cognitive impairment in Alzheimer's disease: investigative and therapeutic perspectives. *J Neurochem.* 1993;60:1589–1604.
12. Baldwin RM, Zea-Ponce Y, Zoghbi SS, et al. Evaluation of the monoamine uptake site ligand [^{123}I]methyl 3 β-(4-iodophenyl)-tropane-2 β-carboxylate ([^{123}I]β-CIT) in non-human primates: pharmacokinetics, biodistribution and SPECT brain imaging coregistered with MRI. *Nucl Med Biol.* 1993;20:597–606.
13. Shih WJ, Schleenbaker RE, Stipp V, Magoun S, Slevin JT. Surface and volume three-dimensional displays of Tc-99m HMPAO brain SPECT images in stroke patients by a three-headed gamma camera. *Clin Nucl Med.* 1993;18:945–949.
14. Kish SJ, Shannak K, Hornykiewicz O. Uneven pattern of dopamine loss in the striatum of patients with idiopathic Parkinson's disease. Pathophysiologic and clinical implications. *N Engl J Med.* 1988;318:876–880.
15. Ichise M, Ballinger JR, Tanaka F, et al. Age-related changes in D2 receptor binding with iodine-123-IBF SPECT. *J Nucl Med.* 1998;39:1511–1518.
16. Talairach J, Tournoux P, Rayport M. *Co-planar Stereotaxic Atlas of the Human Brain. 3-Dimensional Proportional System: An Approach to Cerebral Imaging.* New York, NY: Thieme Inc.; 1988:1–122.
17. Discriminant function analysis. In: *STATISTICA for Windows.* Tulsa, OK: StatSoft, Inc.; 1996:3059–3096.
18. Hughes AJ, Daniel SE, Blankson S, Lees AJ. A clinicopathologic study of 100 cases of Parkinson's disease. *Arch Neurol.* 1993;50:140–148.
19. Rajput AH, Rozdilsky B, Rajput A. Accuracy of clinical diagnosis in parkinsonism—a prospective study. *Can J Neurol Sci.* 1991;18:275–278.
20. Messa C, Lucignani G, Carpinelli A, et al. Characterization of [^{123}I]β-CIT basal ganglia distribution in PD and PSP [abstract]. *J Nucl Med.* 1996;37:133P.
21. Seibyl J, Marek KL, Scheff K, Innis RB. [^{123}I]β-CIT SPECT imaging of dopamine transporters in Parkinson's disease and parkinson syndrome [abstract]. *J Nucl Med.* 1996;37:134P.
22. van Royen E, Verhoeff NF, Speelman JD, Wolters EC, Kuiper MA, Janssen AG. Multiple system atrophy and progressive supranuclear palsy. Diminished striatal D2 dopamine receptor activity demonstrated by ^{123}I-IBZM single photon emission computed tomography. *Arch Neurol.* 1993;50:513–516.
23. Laulumaa V, Kuikka JT, Soininen H, Bergstrom K, Lansimies E, Riekkinen P.

Imaging of D2 dopamine receptors of patients with Parkinson's disease using single photon emission computed tomography and iodobenzamide I-123. *Arch Neurol.* 1993;50:509–512.
24. Gimenez-Roldan S, Mateo D. Cinnarizine-induced parkinsonism. Susceptibility related to aging and essential tremor. *Clin Neuropharmacol.* 1991;14:156–164.
25. Burn DJ, Brooks DJ. Nigral dysfunction in drug-induced parkinsonism: an ^{18}F-dopa PET study. *Neurology.* 1993;43:552–556.
26. Brooks DJ. PET studies in progressive supranuclear palsy. *J Neural Transm.* 1994;42(suppl):119–134.
27. Van Dyck CH, Seibyl JP, Malison RT, et al. Age-related decline in striatal dopamine transporter binding with iodine-123-β-CIT SPECT. *J Nucl Med.* 1995;36:1175–1181.
28. Morrish PK, Sawle GV, Brooks DJ. Regional changes in [^{18}F]dopa metabolism in the striatum in Parkinson's disease. *Brain.* 1996;119:2097–2103.